Journal of Materials Chemistry A

PAPER

View Article Online
View Journal | View Issue

Cite this: J. Mater. Chem. A, 2015, 3, 3130

Efficient polymer solar cells based on a new benzo[1,2-*b*:4,5-*b*′]dithiophene derivative with fluorinated alkoxyphenyl side chain†

Weichao Chen,‡[a] Zhengkun Du,‡[a] Liangliang Han,*[a] Manjun Xiao,[a] Wenfei Shen,[a] Ting Wang,[a] Yuanhang Zhou[a] and Renqiang Yang*[ab]

Received 21st November 2014
Accepted 11th December 2014

DOI: 10.1039/c4ta06350c

www.rsc.org/MaterialsA

A novel fluorine-containing benzo[1,2-*b*:4,5-*b*′]dithiophene (BDT) derivative (BDTPF) was designed to construct a donor–acceptor (D–A)-structured polymer (PBDTPF-DTBT) with the electron-withdrawing unit 4,7-di(4-(2-ethylhexyl)-2-thienyl)-2,1,3-benzothiadiazole (DTBT). The resulting polymer exhibits a broad absorption spectrum, relatively low lying HOMO energy level (−5.39 eV) and a good film-forming ability. The field-effect mobility of PBDTPF-DTBT is 0.034 $cm^2 V^{-1} s^{-1}$. Bulk heterojunction organic solar cells (OSCs) based on PBDTPF-DTBT and $PC_{71}BM$ were prepared and showed a good photovoltaic performance with power conversion efficiency (PCE) of 7.02%. This work demonstrates that a BDT unit with fluorinated alkoxyphenyl side chains is a promising candidate as an electron-rich building block for high performance solution-processed OSCs.

1 Introduction

In the past two decades, solution-processed organic solar cells (OSCs) based on conjugated polymers have attracted considerable attention due to their advantages of light weight, low cost and tunable flexibility. To date, bulk heterojuction (BHJ) OSCs based on copolymers have been well studied and high power conversion efficiencies (PCEs) of over 9% have been achieved, which is mainly attributed to the introduction of novel donor–acceptor (D–A) polymers.[1–8] At present, for large scale commercialization of BHJ polymer solar cells (PSCs), one of the most important issues is the design and synthesis of new solution-processed low band-gap copolymers.[9,10]

The appropriate energy levels, broad absorption spectrum and high charge carrier mobility are of great importance for an ideal donor material, which will directly affect open-circuit voltage (V_{oc}), short-circuit current density (J_{sc}) and fill factor (FF) of solar cells.[9–14] The low lying highest occupied molecular orbital (HOMO) energy level of the donor is usually beneficial for obtaining a high V_{oc}, which is mainly dependent on the offset between the HOMO energy level of the donor and the lowest unoccupied molecular orbital (LUMO) energy level of the acceptor.[15–17] Otherwise, the J_{sc} and FF could be further enhanced by increasing inter-molecular interactions such as π–π stacking.

Benzo[1,2-*b*:4,5-*b*′]dithiophene (BDT) is a good electron-donating unit with a large planar structure, and has received considerable attention to construct D–A polymers for highly efficient OSCs.[18–23] Among the variety of BDT-based electron donor materials, alkylthiophene substituted BDT (BDTT) and phenyl substituted BDT (BDTP) are the main two-dimensional (2D) BDT derivatives with large π-conjugated side chains and high planarity.[24–30] The incorporation of thienyl or phenyl side chains on BDT could extend the perpendicular π–π conjugation and further promote π–π stacking, which could improve charge carrier transport and collection, leading to an improved J_{sc} and FF.[22,24] Compared to its one-dimensional (1D) counterparts, the conjugated polymers based on 2D monomers show a relatively better device performance.[22,24,27,28,31,32] Moreover, the thiophene side chain in the BDTT unit can also be further modified by the introduction of an alkylthio group or a fluorine atom, resulting in a deeper HOMO and higher PCE than those based on the alkyl substituted BDTT with the same electron-deficient acceptor.[3,28,33] Unlike the thiophene unit, the benzene ring exhibits better symmetric structure and weaker electron-donating ability. At present, however, the modification of phenyl substituted BDT is still rare. A comprehensive survey indicates the *meta*-alkoxy-phenyl substituted D–A polymers exhibit higher V_{oc} and PCE compared to *para*-alkoxy-phenyls when the alkoxy-phenyl is connected to the acceptor unit, according to Wang's work.[34,35] The *meta*-alkyloxy-phenyl side-chains result in a more twisted backbone and offer high photovoltaic performance. However, a wider band gap could be obtained when the alkoxy-phenyl is connected to the donor

[a]CAS Key Laboratory of Bio-based Materials, Qingdao Institute of Bioenergy and Bioprocess Technology, Chinese Academy of Sciences, Qingdao 266101, China. E-mail: hanll@qibebt.ac.cn; yangrq@qibebt.ac.cn

[b]State Key Laboratory of Luminescent Materials and Devices, South China University of Technology, Guangzhou 510641, China

† Electronic supplementary information (ESI) available. See DOI: 10.1039/c4ta06350c

‡ W. Chen and Z. Du contributed equally to this work.

unit, according to Hou's report.[27] Therefore, *para*-alkoxy-phenyl is expected to avoid the blue-shifted absorption because of its strong electron donating ability, and the design of a *para*-alkoxy substituted BDTP derivative could be an effective strategy to achieve wide absorption polymers. In addition, in order to obtain a higher V_{oc}, a fluorine atom is always employed to guarantee high hole mobility and deeper HOMO energy level.[36–39] The introduction of fluorine into the conjugated backbone could lower both the LUMO and HOMO energy levels of the conjugated polymers theoretically[40] and experimentally,[22,41] and simultaneously improved V_{oc}, J_{sc} and FF are obtained in their PSCs because of the strong inductive electron-withdrawing property, slight bulkiness and strong F···H/F···S interactions of fluorine.

In this study, a novel 2D BDT monomer containing fluorine atoms (BDTPF) was designed and synthesized by incorporating a fluorine atom at the *meta*-position of the phenyl group. The target polymer, named PBDTPF-DTBT, was obtained using a Pd-catalyzed Stille coupling reaction between the BDTPF and the 4,7-di(4-(2-ethylhexyl)-2-thienyl)-2,1,3-benzothiadiazole (DTBT) unit. The resulting polymer showed a good thermal stability, a deep HOMO energy level of −5.39 eV, and a broad absorption spectrum (350–700 nm). The hole mobility of the PBDTPF-DTBT-based organic thin film transistors (OTFTs) reached 0.034 $cm^2\ V^{-1}\ s^{-1}$. The optimized organic solar cells using PBDTPF-DTBT as donor and [6,6]-phenyl C_{71}-butyric acid methyl ester ($PC_{71}BM$) as acceptor demonstrated a PCE of 7.02% with a high V_{oc} of 0.82 V, a J_{sc} of 13.11 mA cm^{-2} and FF of 65.28% under the illumination of AM 1.5G, 100 mW cm^{-2}.

2 Experimental section

2.1 Materials and reagents

All starting materials and reagents were purchased from commercial sources and used without further purification. Toluene was distilled over sodium and was freshly distilled prior to use. The synthetic routes for the monomers and copolymer are shown in Scheme 1. Benzo[1,2-*b*:4,5-*b*′]dithiophene-4,8-dione and **M2** were synthesized according to the reported methods.[42,43] The detailed synthetic routes for **M1** and the polymer are as follows.

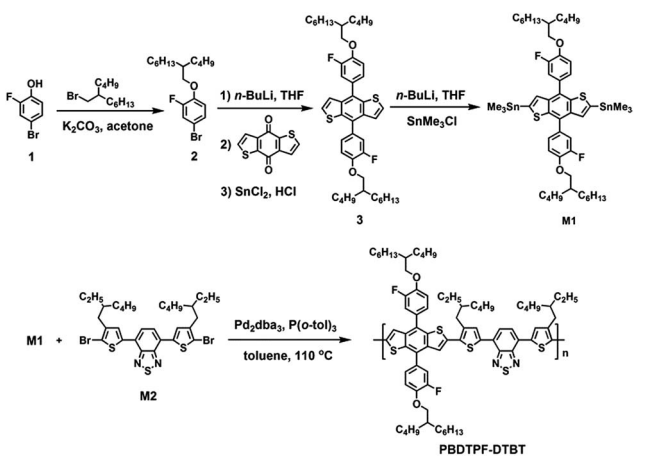

Scheme 1 Synthetic route and molecular structure of the polymer PBDTPF-DTBT.

Synthesis of compound 2. A stirred mixture of 4-bromo-2-fluorophenol (4.78 g, 25 mmol), 5-(bromomethyl)undecane (6.85 g, 27.5 mmol), dry acetone (30 mL) and anhydrous potassium carbonate (7.6 g, 55 mmol) was heated at 75 °C for 24 h. Thereafter, the cooled reaction mixture was filtered to remove inorganic salts and then the acetone phase was poured into water (50 mL). The mixture was extracted three times with diethyl ether. The combined organic phase was washed with water twice and then dried over magnesium sulfate. After filtration, the solvent was removed under vacuum and the crude product was purified on a silica gel column eluting with petroleum ether. A pale yellow oil, compound **2**, was obtained (7.18 g, 80% yield). ^{1}H NMR (600 MHz, $CDCl_3$), δ (ppm): 7.22 (dd, 1H), 7.16 (d, 1H), 6.82 (t, 1H), 3.86 (d, 2H), 1.80 (m, 1H), 1.48–1.27 (m, 16H), 0.91–0.87 (m, 6H). ^{13}C NMR (150 MHz, $CDCl_3$), δ (ppm): 153.54, 151.88, 146.95, 146.88, 127.11, 127.08, 119.70, 119.56, 116.07, 116.06, 111.70, 111.64. 72.64, 37.91, 31.83, 31.21, 30.89, 29.64, 29.00, 26.76, 23.02, 22.67, 14.10, 14.07.

Synthesis of compound 3. In an inert atmosphere of argon, compound **2** (6.46 g, 18 mmol) was dissolved in dry THF (40 mL) and then *n*-butyllithium solution (18 mmol, 11.25 mL, 1.6 M in *n*-hexane) was added dropwise at −78 °C. After addition, the reaction mixture was maintained at −78 °C for 1 h, followed by the addition of benzo[1,2-*b*:4,5-*b*′]dithiophene-4,8-dione (1.32 g, 6 mmol) and allowed to warm to 55 °C for 2 h. The solution was cooled down and then $SnCl_2 \cdot 2H_2O$ (10.83 g, 48 mmol) in 10% aqueous HCl (12.5 mL) was added. The solution was refluxed for 2 h and then the cooled mixture was poured into water and extracted with diethyl ether. The combined organic phase was dried over magnesium sulfate and evaporated to obtain the crude product, which was purified on a silica gel column, eluting with petroleum ether and dichloromethane. Compound **3** was obtained as a pale yellow oil (1.57 g, 35% yield). ^{1}H NMR (600 MHz, $CDCl_3$), δ (ppm): 7.44–7.39 (m, 6H), 7.33 (d, 2H), 7.14 (t, 2H), 4.02 (d, 4H), 1.90 (m, 2H), 1.54–1.32 (m, 32H), 0.95–0.89 (m, 12H). ^{13}C NMR (150 MHz, $CDCl_3$), δ (ppm): 153.51, 151.87, 147.46, 147.39, 138.24, 136.14, 131.75, 131.71, 129.16, 127.44, 125.26, 125.24, 122.81, 117.31, 117.18, 114.88, 72.40, 38.04, 31.88, 31.33, 31.02, 29.71, 29.08, 26.84, 23.08, 22.71, 14.14, 14.12.

Synthesis of compound M1. In an inert atmosphere of argon, a solution of compound **3** (1.12 g, 1.5 mmol) was dissolved in dry THF (30 mL), and then, *n*-butyllithium solution (4.13 mmol, 2.58 mL, 1.6 M in *n*-hexane) was added dropwise at 0 °C. Then the mixture was maintained at 0 °C for 1.5 h and trimethyltin chloride solution (4.7 mmol, 4.7 mL, 1.0 M in *n*-hexane) was added at 0 °C. The solution was stirred overnight and poured into water. The mixture was extracted three times with diethyl ether and the combined organic phase was dried over magnesium sulfate. After removing the solvents, the crude product was recrystallized from isopropanol to afford a pale yellow solid **M1** (0.96 g, 60% yield). ^{1}H NMR (600 MHz, $CDCl_3$), δ (ppm): 7.46–7.41 (m, 4H), 7.35 (s, 2H), 7.15 (t, 2H), 4.03 (d, 4H), 1.90 (m, 2H), 1.54–1.32 (m, 32H),

0.94 (t, 6H), 0.91 (m, 6H), 0.37 (s, 18H). ^{13}C NMR (150 MHz, $CDCl_3$), δ (ppm): 153.46, 151.82, 147.25, 147.18, 142.53, 142.36, 136.97, 132.44, 132.39, 130.45, 127.57, 125.32, 125.30, 117.39, 117.26, 114.76, 72.31, 38.07, 31.89, 31.35, 31.04, 29.71, 29.10, 26.86, 23.09, 22.71, 14.14, 14.13, −8.34.

Synthesis of PBDTPF-DTBT. Compound **M1** (0.27 g, 0.25 mmol), **M2** (0.17 g, 0.25 mmol) and 7 mL of dry toluene were put into a two-necked flask. The flask was purged three times with successive vacuum and argon filling cycles, and then, Pd_2dba_3 (3.7 mg) and P(*o*-tol)$_3$ (7.3 mg) were added into the flask. The solution was heated to 110 °C carefully and stirred overnight at this temperature under argon protection. The reaction was cooled to room temperature and then poured into methanol (125 mL) slowly. The polymer was filtered and purified by Soxhlet extraction with methanol, acetone, hexane and chloroform. The polymer was obtained from the chloroform fraction after the evaporation of the solvent as a black-blue solid (142 mg, 45% yield). M_n = 13.9 kDa, PDI = 2.3.

2.2 Fabrication and characterization of devices

Organic solar cells were fabricated with the structure ITO/PEDOT : PSS/PBDTPF-DTBT : $PC_{71}BM$/Ca/Al. Patterned ITO-coated glass was cleaned with ITO detergent, deionized water, acetone and isopropanol in an ultrasonic bath for 20 min each time and then exposed to oxygen plasma for 6 min. PEDOT : PSS (Baytron PVP Al 4083) was spin-coated onto ITO-coated glass substrates, followed by annealing at 160 °C for 30 minutes. Subsequently, the substrates were transferred to a glove box. The active layer consisting of polymers and $PC_{71}BM$ was spin-coated from *o*-dichlorobenzene (*o*-DCB) solution (30 mg mL^{-1}) onto the PEDOT : PSS layer. The spin-coating was operated in a glove box. Finally, after the samples were transferred to a vacuum chamber, Ca (10 nm) and Al (100 nm) were deposited *via* a mask to define the active area of 0.10 cm^2 in high vacuum.

The OFET was fabricated using the n-type heavily doped Si as a gate with a 300 nm thermally oxidized SiO_2 layer as gate dielectric (the capacitance is 10 nF cm^{-2}). The film was prepared by spin-coating the solution (16 mg mL^{-1} in *o*-DCB) on octadecyltrichlorosilane (OTS)-treated SiO_2/Si. The Au source and drain electrodes were deposited on the film through a shadow mask with a length of 31 μm and a width of 273 μm. Measurements were performed using a 4200 semiconductor parameter analyzer in air.

Atomic force microscopy (AFM) measurements of film morphology were imaged by an Agilent 5400 with tapping mode. Transmission electron microscopy (TEM) images were obtained on a JEOL JEM-1011 transmission electron microscope at an accelerating voltage of 100 kV.

PCE was calculated from current density–voltage (*J*–*V*) curves, which were recorded by a Keithley 2420 source meter under an illumination of an AM 1.5G solar simulator with an intensity of 100 mW cm^{-2}. The light intensity was calibrated by a standard silicon photodiode. EQE of solar cells were analyzed using a certified Newport incident photon conversion efficiency (IPCE) measurement system.

3 Results and discussion

3.1 Synthesis and characterization

The general synthetic routes for the monomer BDTPF and the target polymer PBDTPF-DTBT are shown in Scheme 1. The chemical structure of monomer **M1** was characterized by ^{1}H NMR and ^{13}C NMR spectra (Fig. S5†). Polymer PBDTPF-DTBT was synthesized by the Stille coupling reaction in refluxing toluene under argon for 12 h. The detailed synthesis is given in the Experimental section. The number average molecular weight (M_n) of PBDTPF-DTBT was measured at 13.9 kDa with a polydispersity index (PDI) of 2.3. The thermal properties of the polymer were measured by thermogravimetric analysis (TGA) in a nitrogen atmosphere at a heating rate of 10 °C min^{-1}. The polymer exhibited a high thermal stability with onset decomposition temperature with 5% weight-loss (T_d) located at 443 °C as shown in Fig. S1.†

3.2 Optical and electrochemical properties

The normalized absorption spectra of PBDTPF-DTBT in chloroform solution and as the thin film are shown in Fig. 1(a). PBDTPF-DTBT exhibits two absorption bands between 350 nm and 700 nm both in chloroform and in the solid state. The PBDTPF-DTBT solution displays two main absorption peaks, which are at 420 nm and 576 nm and a shoulder peak at about 650 nm. Similar to the absorption in solution, the

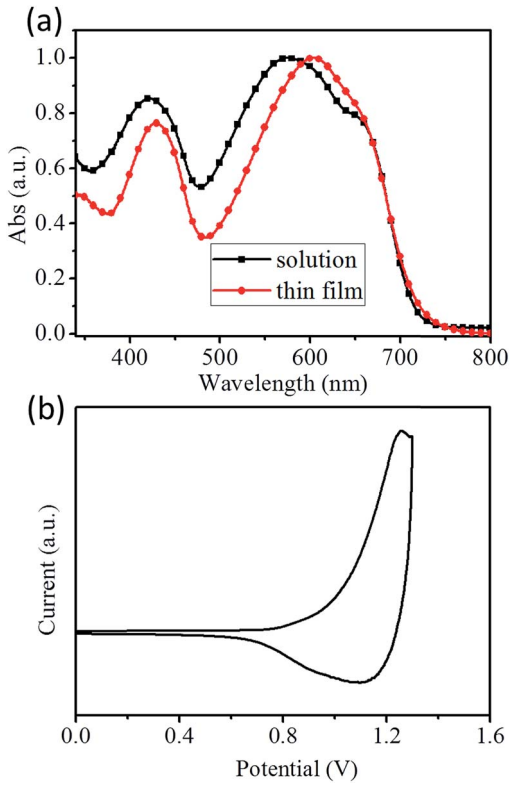

Fig. 1 (a) UV-vis absorption spectra of the polymer in chloroform solution and as the solid film. (b) Cyclic voltammogram of as casted film *vs.* the SCE in 0.1 M Bu_4NPF_6/acetonitrile solution.

PBDTPF-DTBT film also shows two absorption peaks at 430 nm and 635 nm. Although the PBDTPF-DTBT film has more red-shifted peaks compared to the solution, the solution shows the broader absorption range, which could be ascribed to the molecular aggregates in the solution.[31,44] The optical band gap is around 1.73 eV, calculated from the absorption edge (715 nm) of the thin film.

The cyclic voltammetry (CV) measurements were performed to investigate the electrochemical properties of PBDTPF-DTBT. As shown in Fig. 1(b), the onset potential of the oxidation wave of PBDTPF-DTBT is 0.98 V *versus* the standard saturated calomel electrode (SCE), corresponding to the HOMO energy level of −5.39 eV. The LUMO energy level calculated from the HOMO and optical band gap is about −3.66 eV. The high V_{oc} of solution-processed OSCs based on PBDTPF-DTBT and $PC_{71}BM$ could be expected due to the relatively low HOMO energy level of PBDTPF-DTBT.[45]

3.3 Hole mobility

The carrier charge mobility is an important parameter, which could affect charge separation of the exciton, charge carrier transport and recombination.[46] The mobility of PBDTPF-DTBT was investigated by employing OFETs and vertical diodes. Fig. S2† shows the output characteristics, which exhibited a typical p-type semiconductor behavior. The hole mobility was around 0.034 $cm^2\ V^{-1}\ s^{-1}$, calculated according to the transfer characteristic curve at $V_{GS} = -60$ V, as shown in Fig. S2.† In the vertical direction, the hole mobility was measured using a vertical diode with the device structure of ITO/PEDOT : PSS/PBDTPF-DTBT/Au. According to the *J*–*V* curve, as shown in Fig. S3,† the mobility is about $1.5 \times 10^{-5}\ cm^2\ V^{-1}\ s^{-1}$, calculated using a space-charge-limited-current (SCLC) model,[47] which is described by the equation $J_{SCLC} = (9/8)\ \varepsilon_0\varepsilon_r\mu_h((V^2)/(L^3))$, where *J* stands for current density, ε_0 is the permittivity of free space, ε_r is the relative dielectric constant of the transport medium, μ_h is the hole mobility, *V* is the internal potential in the device and *L* is the thickness of the active layer.

3.4 Photovoltaic properties

To investigate the photovoltaic properties of PBDTPF-DTBT, conventional BHJ solar cells were fabricated with $PC_{71}BM$ as acceptor. The devices with the structure of glass/ITO/PEDOT : PSS/PBDTPF-DTBT : $PC_{71}BM$/Ca/Al were tested under the illumination of AM 1.5G simulated solar lights (100 mW cm^{-2}). The devices with different D/A weight ratios (PBDTPF-DTBT/$PC_{71}BM$) were fabricated to optimize the device. The *J*–*V* curves of the devices with the D/A ratios of 1.5 : 1, 1 : 1, 1 : 1.5 and 1 : 2 are shown in Fig. S4.† Evidently, the optimal D/A ratio is 1 : 1, and a PCE of 4.35% was obtained with $V_{oc} = 0.85$ V, $J_{sc} = 10.84$ mA cm^{-2} and FF = 47.16%. 1,8-Diiodooctane (DIO) was used to further improve the photovoltaic performance, and the corresponding photovoltaic parameters of the devices with different DIO ratios are summarized in Table 1. Fig. 2 shows the typical *J*–*V* and EQE curves of solar cells based on the PBDTPF-DTBT/$PC_{71}BM$ (1 : 1, w/w) blend spin-coated without additive and with 0.5% DIO (DIO/*o*-DCB, v/v). The optimal PCE of 7.02% was obtained with $V_{oc} = 0.82$ V, $J_{sc} = 13.11$ mA cm^{-2}, and FF = 65.28% when using 0.5% DIO as the solvent additive, as shown in Fig. 2(a). Compared to the device processed without additive, the device processed with DIO showed higher EQE covering a wide range and therefore resulted in a higher J_{sc}. The current density obtained by integrating the EQE curve of the device with the standard AM 1.5G solar spectrum is about 12.51 mA cm^{-2}, which is slightly smaller than the measured value (13.11 mA cm^{-2}) with the error <5%. Moreover, FF also remarkably improved from 47.16% to 65.28%. Compared with the similar copolymers without F atoms on the

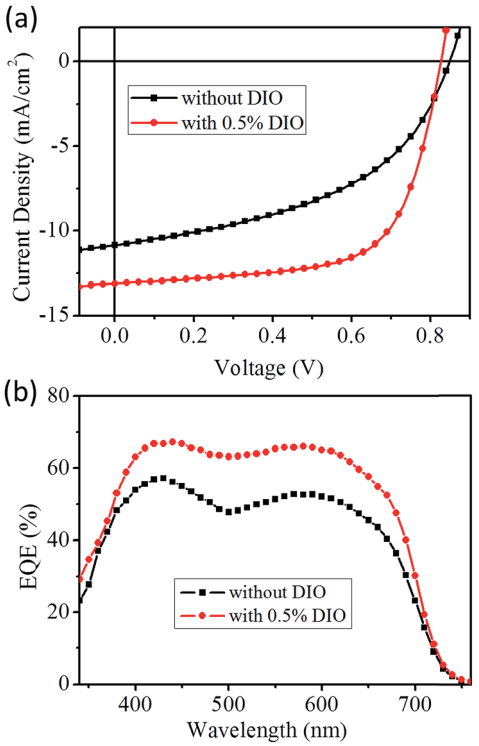

Fig. 2 (a) The *J*–*V* curves and (b) EQE spectra of PBDTPF-DTBT : $PC_{71}BM$ (1 : 1, w/w) devices with and without DIO.

Table 1 Photovoltaic properties of the devices based on PBDTPF-DTBT and $PC_{71}BM$ (1 : 1, w/w) under illumination of AM 1.5G, 100 mW cm^{-2}

Donor/acceptor	DIO (v/v)	V_{oc} (V)	J_{sc} (mA cm^{-2})	FF (%)	PCE_{max}/PCE_{ave}[a] (%)
PBDTPF-DTBT/$PC_{71}BM$ (1 : 1, w/w)	0	0.85	10.84	47.16	4.35/4.21
	0.5%	0.82	13.11	65.28	7.02/6.90
	1%	0.82	11.46	59.43	5.58/5.39

[a] The average PCE was obtained from over 10 devices.

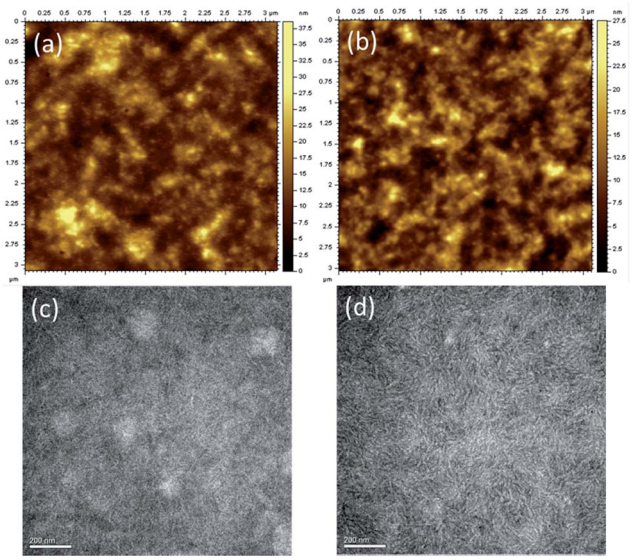

Fig. 3 The AFM and TEM images of PBDTPF-DTBT : $PC_{71}BM$ films with and without DIO. (a) AFM image without DIO, (b) AFM image with 0.5% DIO, (c) TEM image without DIO and (d) TEM image with 0.5% DIO.

benzene ring for solar cells, the optimal devices based on PBDTPF-DTBT exhibited higher V_{oc} and J_{sc}.[29]

3.5 Morphology

The influence of DIO on the surface morphologies of the blended films was investigated by AFM and TEM. As shown in Fig. 3(a), the surface of the film processed by *o*-DCB is non-uniform with root-mean-square (RMS) roughness value of *ca.* 4.8 nm because of relatively large domains on the surface, whereas after adding 0.5% DIO, the film became uniform with a relatively lower RMS value of *ca.* 3.5 nm (Fig. 3(b)). However, the scale of the dark and light domains, which correspond to the aggregations of polymer and $PC_{71}BM$ respectively, became evident after adding 0.5% DIO as shown in Fig. 3(c) and (d). This indicates that the phase separation of polymer and $PC_{71}BM$ is enhanced, and therefore, the interpenetrating network may be formed under the assistance of DIO. This could enhance the transport and collection of charge carriers, which resulted in the improvement of J_{sc} and FF.

4 Conclusion

A new solution-processed polymer, named PBDTPF-DTBT, was designed and synthesized using a fluorine-containing BDTP derivative (BDTPF) with DTBT. The resulting polymer showed high thermal stability, broad absorption spectra, a relatively low lying HOMO energy level and good film-forming ability. The device based on PBDTPF-DTBT and $PC_{71}BM$ exhibited good photovoltaic performance with PCE = 7.02%, V_{oc} = 0.82 V, J_{sc} = 13.11 mA cm^{-2} and FF = 65.28%. The results demonstrate that a BDT unit containing fluorinated alkoxyphenyl side chains may be a promising electron-donor building block for high performance solution-processed OSCs.

Acknowledgements

This work was supported by the Ministry of Science and Technology of China (2014CB643501, 2010DFA52310), the National Natural Science Foundation of China (61405209, 51303197, 51211140346, 51173199, 21274161), and the Qingdao Municipal Science and Technology Program (11-2-4-22-hz).

Notes and references

1 C. C. Chen, W. H. Chang, K. Yoshimura, K. Ohya, J. B. You, J. Gao, Z. Hong and Y. Yang, *Adv. Mater.*, 2014, **26**, 5670.
2 Z. C. He, C. M. Zhong, S. J. Su, M. Xu, H. B. Wu and Y. Cao, *Nat. Photonics*, 2012, **6**, 591.
3 L. Ye, S. Q. Zhang, W. C. Zhao, H. F. Yao and J. H. Hou, *Chem. Mater.*, 2014, **26**, 3603.
4 J. B. You, L. T. Dou, K. Yoshimura, T. Kato, K. Ohya, T. Moriarty, K. Emery, C. C. Chen, J. Gao, G. Li and Y. Yang, *Nat. Commun.*, 2013, **4**, 1446.
5 M. Yusoff, A. Rashid bin, D. Kim, H. Kim, F. K. Shneider, W. da Silva and J. Jang, *Energy Environ. Sci.*, 2015, **8**, 303.
6 T. L. Nguyen, H. Choi, S. J. Ko, M. A. Uddin, B. Walker, S. Yum, J. E. Jeong, M. H. Yun, T. J. Shin, S. Hwang, J. Y. Kim and H. Y. Woo, *Energy Environ. Sci.*, 2014, **7**, 3040.
7 S. H. Liao, H. J. Jhuo, P. N. Yeh, Y. S. Cheng, Y. Li, Y. H. Lee, S. Sharma and S. A. Chen, *Sci. Rep.*, 2014, **4**, 6318.
8 Y. Liu, J. Zhao, Z. Li, C. Mu, W. Ma, H. Hu, K. Jiang, H. Lin, H. Ade and H. Yan, *Nat. Commun.*, 2014, **5**, 5293.
9 J. W. Chen and Y. Cao, *Acc. Chem. Res.*, 2009, **42**, 1709.
10 Y. F. Li, *Acc. Chem. Res.*, 2012, **45**, 723.
11 K. A. Mazzio and C. K. Luscombe, *Chem. Soc. Rev.*, 2015, **44**, 78.
12 Z. B. Henson, K. Mullen and G. C. Bazan, *Nat. Chem.*, 2012, **4**, 699.
13 X. Guo, M. Baumgarten and K. Mullen, *Prog. Polym. Sci.*, 2013, **38**, 1832.
14 C. H. Duan, F. Huang and Y. Cao, *J. Mater. Chem.*, 2012, **22**, 10416.
15 C. J. Brabec, A. Cravino, D. Meissner, N. S. Sariciftci, T. Fromherz, M. T. Rispens, L. Sanchez and J. C. Hummelen, *Adv. Funct. Mater.*, 2001, **11**, 374.
16 M. C. Scharber, D. Wuhlbacher, M. Koppe, P. Denk, C. Waldauf, A. J. Heeger and C. L. Brabec, *Adv. Mater.*, 2006, **18**, 789.
17 A. J. Heeger, *Adv. Mater.*, 2014, **26**, 10.
18 J. H. Hou, M. H. Park, S. Q. Zhang, Y. Yao, L. M. Chen, J. H. Li and Y. Yang, *Macromolecules*, 2008, **41**, 6012.
19 D. Lee, S. W. Stone and J. P. Ferraris, *Chem. Commun.*, 2011, **47**, 10987.
20 Y. Y. Liang, Z. Xu, J. B. Xia, S. T. Tsai, Y. Wu, G. Li, C. Ray and L. P. Yu, *Adv. Mater.*, 2010, **22**, E135.
21 C. Cabanetos, A. El Labban, J. A. Bartelt, J. D. Douglas, W. R. Mateker, J. M. J. Frechet, M. D. McGehee and P. M. Beaujuge, *J. Am. Chem. Soc.*, 2013, **135**, 4656.
22 L. Ye, S. Q. Zhang, L. J. Huo, M. J. Zhang and J. H. Hou, *Acc. Chem. Res.*, 2014, **47**, 1595.

23 N. Wang, Z. Chen, W. Wei and Z. Jiang, *J. Am. Chem. Soc.*, 2013, **135**, 17060.
24 L. J. Huo, S. Q. Zhang, X. Guo, F. Xu, Y. F. Li and J. H. Hou, *Angew. Chem., Int. Ed.*, 2011, **50**, 9697.
25 M. J. Zhang, Y. Gu, X. Guo, F. Liu, S. Q. Zhang, L. J. Huo, T. P. Russell and J. H. Hou, *Adv. Mater.*, 2013, **25**, 4944.
26 L. T. Dou, J. Gao, E. Richard, J. B. You, C. C. Chen, K. C. Cha, Y. J. He, G. Li and Y. Yang, *J. Am. Chem. Soc.*, 2012, **134**, 10071.
27 M. J. Zhang, X. Guo, W. Ma, S. Q. Zhang, L. J. Huo, H. Ade and J. H. Hou, *Adv. Mater.*, 2014, **26**, 2089.
28 C. Cui, W. Wong and Y. Li, *Energy Environ. Sci.*, 2014, **7**, 2276.
29 M. C. Hwang, H. Kang, K. Yu, H. J. Yun, S. K. Kwon, K. Lee and Y. H. Kim, *Sol. Energy Mater. Sol. Cells*, 2014, **125**, 39.
30 L. L. Han, X. C. Bao, T. Hu, Z. K. Du, W. C. Chen, D. Q. Zhu, Q. Liu, M. L. Sun and R. Q. Yang, *Macromol. Rapid Commun.*, 2014, **35**, 1153.
31 D. P. Qian, L. Ye, M. J. Zhang, Y. R. Liang, L. J. Li, Y. Huang, X. Guo, S. Q. Zhang, Z. A. Tan and J. H. Hou, *Macromolecules*, 2012, **45**, 9611.
32 J. Y. Yuan, H. L. Dong, M. Li, X. D. Huang, J. Zhong, Y. Y. Li and W. L. Ma, *Adv. Mater.*, 2014, **26**, 3624.
33 M. J. Zhang, X. Guo, S. Q. Zhang and J. H. Hou, *Adv. Mater.*, 2014, **26**, 1118.
34 E. G. Wang, J. Bergqvist, K. Vandewal, Z. F. Ma, L. T. Hou, A. Lundin, S. Himmelberger, A. Salleo, C. Muller, O. Inganas, F. L. Zhang and M. R. Andersson, *Adv. Energy Mater.*, 2013, **3**, 806.
35 D. F. Dang, W. C. Chen, S. Himmelberger, Q. Tao, A. Lundin, R. Q. Yang, W. G. Zhu, A. Salleo, C. Muller and E. G. Wang, *Adv. Energy Mater.*, 2014, **4**, 1400680.
36 D. F. Dang, W. C. Chen, R. Q. Yang, W. G. Zhu, W. Mammo and E. G. Wang, *Chem. Commun.*, 2013, **49**, 9335.
37 H. X. Zhou, L. Q. Yang, A. C. Stuart, S. C. Price, S. B. Liu and W. You, *Angew. Chem., Int. Ed.*, 2011, **50**, 2995.
38 Y. Y. Liang, Z. Xu, J. B. Xia, S. T. Tsai, Y. Wu, G. Li, C. Ray and L. P. Yu, *Adv. Mater.*, 2010, **22**, E135.
39 S. C. Price, A. C. Stuart, L. Q. Yang, H. X. Zhou and W. You, *J. Am. Chem. Soc.*, 2011, **133**, 4625.
40 J. L. Bredas and A. J. Heeger, *Chem. Phys. Lett.*, 1994, **217**, 507.
41 Y. Y. Liang and L. P. Yu, *Acc. Chem. Res.*, 2010, **43**, 1227.
42 H. X. Zhou, L. Q. Yang, S. Q. Xiao, S. B. Liu and W. You, *Macromolecules*, 2010, **43**, 811.
43 S. C. Lan, P. A. Yang, M. J. Zhu, C. M. Yu, J. M. Jiang and K. H. Wei, *Polym. Chem.*, 2013, **4**, 1132.
44 J. Lee, S. Jo, M. Kim, H. G. Kim, J. Shin, H. Kim and K. Cho, *Adv. Mater.*, 2014, **26**, 6706.
45 Z. K. Du, W. C. Chen, S. G. Wen, S. L. Qiao, Q. Liu, D. Ouyang, N. Wang, X. C. Bao and R. Q. Yang, *ChemSusChem*, 2014, **7**, 3319.
46 T. M. Clarke and J. R. Durrant, *Chem. Rev.*, 2010, **110**, 6736.
47 V. D. Mihailetchi, J. Wildeman and P. W. M. Blom, *Phys. Rev. Lett.*, 2005, **94**, 126602.